Science Advances
AAAS

advances.sciencemag.org/cgi/content/full/6/50/eaba2470/DC1

Supplementary Materials for

DNA methyltransferase 3B deficiency unveils a new pathological mechanism of pulmonary hypertension

Yi Yan, Yang-Yang He, Xin Jiang, Yong Wang, Ji-Wang Chen, Jun-Han Zhao, Jue Ye, Tian-Yu Lian, Xu Zhang, Ru-Jiao Zhang, Dan Lu, Shan-Shan Guo, Xi-Qi Xu, Kai Sun, Su-Qi Li, Lian-Feng Zhang, Xue Zhang, Shu-Yang Zhang, Zhi-Cheng Jing*

*Corresponding author. Email: jingzhicheng@vip.163.com

Published 9 December 2020, *Sci. Adv.* **6**, eaba2470 (2020)
DOI: 10.1126/sciadv.aba2470

This PDF file includes:

Materials and Methods

Animal models

All animal protocols were approved by the Ethics and Animal Care and Use Committee of FuWai hospital and Beijing Shijitan hospital or the University of Illinois at Chicago. All animal work was carried out in accordance with the relevant guidelines and regulations of these bodies.

Rats

All rats used in this work possessed a Sprague-Dawley background. To test the DNA methyltransferases profiling in PH rodent models, male Sprague-Dawley rats (~250 to 300 g) were purchased from Charles River (Beijing, China). *Dnmt3b*$^{-/-}$ rats were obtained as a generous gift from Professor Lianfeng Zhang from the Institute of Laboratory Animal Science, Chinese Academy of Medical Sciences.

Hypobaric hypoxia — hypobaric hypoxic chambers maintained with a 50 kPa air pressure (equal to that in 5000 m altitude) were opened twice a week for cleaning and replenishment of food and water. And soda lime was used to reduce the concentration of carbon dioxide. For normoxic conditions, rats were kept in the same room with the same 12-hour-light-12-hour-dark cycle. **For wildtype rats experiments (Fig. 1)**, 8-week old male rats were kept in either hypobaric hypoxic chamber or in room air (21% oxygen) continuously for 3 weeks, and then animals were sacrificed for analysis. **For knockout rats experiments (Fig. 2-3)**, 8-week old male *Dnmt3b*$^{-/-}$ as well as wildtype male littermates were kept in either hypobaric hypoxic chamber or in room air for 3 weeks.

Monocrotaline — a single subcutaneous injection MCT (Sigma-Aldrich, St. Louis, MO, USA)

or sterile saline was given to male Sprague-Dawley rats to develop PH. **For wildtype rats experiments (Fig. 1)**, 8-week old male rats were assigned to either a single subcutaneous injection of 60 mg/kg of MCT or saline alone. At day 21, rats were sacrificed for analysis. **For knockout rats experiments (Fig. 2-3)**, 8-week old male *Dnmt3b*$^{-/-}$ as well as wildtype male littermates were assigned to either injection of 50 mg/kg of MCT or saline alone. At day 28, animals were sacrificed for analysis.

Mice

To investigate the effect of DNMT3B overexpression on the development of PH (**Fig. 4**), 6 to 8 week old C57BL/6 mice were anesthetized by using an i.p. injection of ketamine (100 mg/kg) and xylazine (10 mg/kg), and then mice were delivered intratracheally with 2 x 10^{11} GC of either AAV9-DNMT3B or AAV9-null in a final solution of 100 μL, the mouse was maintained at a 45° angle for 1 min. Two weeks later mice should be kept in the hypoxia chamber or in normoxia for the additional 2 weeks. At day 28, animals were sacrificed for analysis.

Cell culture

Rat PASMCs were isolated from adult Sprague-Dawley rats. Briefly, the rats were sacrificed, and the lungs were excised from the chest cavity and rinsed with phosphate-buffered saline (PBS). The superficial tissue and the bronchus artery were discarded with fine micro-scissors, and the adventitia was removed from the isolated arteries under a dissecting microscope. Minced arteries were attached to bottom of cell culture dish and then immersed by Dulbecco's modified eagle medium/F12 (DMEM/F12) containing 20% fetal bovine serum (FBS), 100 U/mL penicillin and 100

μg/mL streptomycin in a 37 °C, 5% CO_2 humidified incubator. Three days later, non-adherent cells were removed, and the adherent cells that had grown to 90% confluence were considered as passage 0 PASMCs. Human PASMC were purchased from ScienCell, San Diego, California. Passages 3–4 were used for the subsequent experiments.

siRNA transfection

DNMT3B siRNA and scrambled control sequences were designed and prepared by Invitrogen. Three 25-nucleotide sequences were selected from the ORF sequence of rat DNMT3B (GenBank accession no. NM_001003959.1). The scrambled oligonucleotide served as a nonsilencing control. Suppression of DNMT3B expression by the siRNA oligonucleotides was evaluated in PASMCs using Lipofectamine™ RNAiMAX (Invitrogen) as the transfection reagent following the manufacturer's instructions. 5 h after transfection, cells were changed with fresh complete DMEM/F12 medium, and later used for smooth muscle cell growth assays, migration assay, real time PCR, or protein assays. The efficiency of gene knockdown was assessed by western blotting 48 h after siRNA transfection. Three (siRNA-1, -2, and -3) of the siRNA sequences were evaluated for the efficiency of suppression of DNMT3B protein levels, with siRNA-2 being the most effective (5′-CACAACCAUUGACUUUGCCGCUUCU-3′).

Adenovirus vector constructs and infection

PASMCs were infected with pHBAd-MCMV-GFP adenovirus encoding the cDNA GFP (AdControl) and DNMT3B (AdDNMT3B). For virus infection, PASMCs were plated at ~50%

confluency and infected at multiplicity of infection of 10 or 20 for 24 h. Cells were changed with fresh DMEM/F12 medium containing 5% FBS for additional 24 h, and were then used for smooth muscle cell growth assays or migration assay.

Cell viability and proliferation assays

For nanaomycin A experiments— Rat PASMCs were seeded at 0.8×10^5 cells per well with complete medium in 96-well plate and 24 h later, growth-arrested by washing the cells three times with PBS prior to the addition of DMEM/F12 without FBS. Cells were incubated at 37 °C, 5% CO_2 for 24 h and then treated with vehicle (DMEM/F12 without serum) or PDGF-BB or nanaomycin A or combination of nanaomycin A and PDGF-BB for 48 h. To test cell viability, culture supernatant was discarded and replaced with CCK-8 solution (Dojindo Laboratories, China), and cells were incubated at 37 °C, 5% CO_2 for 1.5 h. Absorbance values (OD) were determined by a microplate reader (Infinite M200 Pro, Tecan, Switzerland) at a wavelength of 450 nm. To test cell proliferation, culture supernatant was discarded and incubated with 0.1% crystal violet for 10 min at room temperature. Washed the plate for 3 times and added 100 μL 0.1% SDS to each well. The plate was gentle shaken to dissolve the dye thoroughly in an enzyme-linked immunosorbent detector. OD value was determined at a wavelength of 570 nm.

For siRNA transfection experiments—Cell viability or proliferation was assessed in rat PASMCs transfected with si*DNMT3B* or scrambled siRNA by CCK-8 assay or crystal violet assay as above, respectively.

For adenovirus infection experiments—Cell viability or proliferation was assessed in rat

PASMCs infected with AdDNMT3B or AdControl by CCK-8 assay or crystal violet assay as above.

Wound-scratch assay

Human

For nanaomycin A experiments, 1.5×10^4 human PASMCs/well were seeded in 96-well plates. A scratch was made on confluent monolayers using a 96-pin WoundMaker™. Cells were left untreated or treated with nanaomycin A (0.3 μM) or vehicle in response to PDGF-BB for 48 h. For adenovirus infection experiments, hPASMCs were seeded at a density of 1×10^4 cells/well and infected with AdDNMT3B or AdControl for 24 h followed by a scratch, and then treated with PDGF-BB or vehicle for 48 h. Cell confluence was imaged by phase contrast using the IncuCyte HD system (IncuCyte™ live-cell). Frames were captured at 6-h intervals from 2 separate regions/well using ×10 objective. Cultures were run in six replicates. Wound images were automatically acquired and registered by IncuCyte Zoom software system. Data were processed and analyzed using IncuCyte Zoom 96-Well Cell Invasion Software Application Module (all from Essen BioScience, Inc., Ann Arbor, MI, USA). Data are presented as the wound confluency.

Rat

For nanaomycin A experiments, rat PASMCs were seeded at 1×10^5 cells per well with complete medium in 12-well plate to form a monolayer. Cells were washed three times with PBS prior to the addition of DMEM/F12 without FBS. 24 h after cell starvation, the monolayers were then scratched with a P200 pipette tip, and cells were washed twice with PBS prior to administration of vehicle (DMEM/F12 without serum) or PDGF-BB or combined treatment of nanaomycin A (0.3 μM) and

PDGF-BB (50 ng/mL). For adenovirus infection experiments, rat PASMCs were infected with AdDNMT3B or AdControl as mentioned above, and then wound-scratch assays were performed as above. Phase-contrast images were obtained at × 100 magnifications at indicated time point post-scratching. Six images of each individual scratch were taken.

Transwell assay

Rat PASMCs were transfected with si*DNMT3B* or Scrambled siRNA and cultured for 48h in complete medium, cells then were starved for 24 h and digested, washed twice with PBS, and suspended in serum free DMEM/F12 medium. The cell density was adjusted to 6×10^4/mL. The experiment was performed in 24-well 8 μm Transwell plates (Corning-Costar, Corning, NY, USA) (3 chambers per group; 100 μL cell suspension per chamber). The lower chamber with the addition of 600 μL DMEM/F12 medium in the presence or absence of PDGF-BB was incubated in 5% CO_2 at 37 °C. 18 h later, cells were fixed with 4% paraformaldehyde for 20 min at room temperature. Chambers were subjected to 0.1% crystal violet dye for 5 min, washed twice with PBS, and then kept dry at temperature overnight before photographing. The number of stained cells was counted under inverted microscope. Five field counts were randomly selected. Three independent experiments were performed.

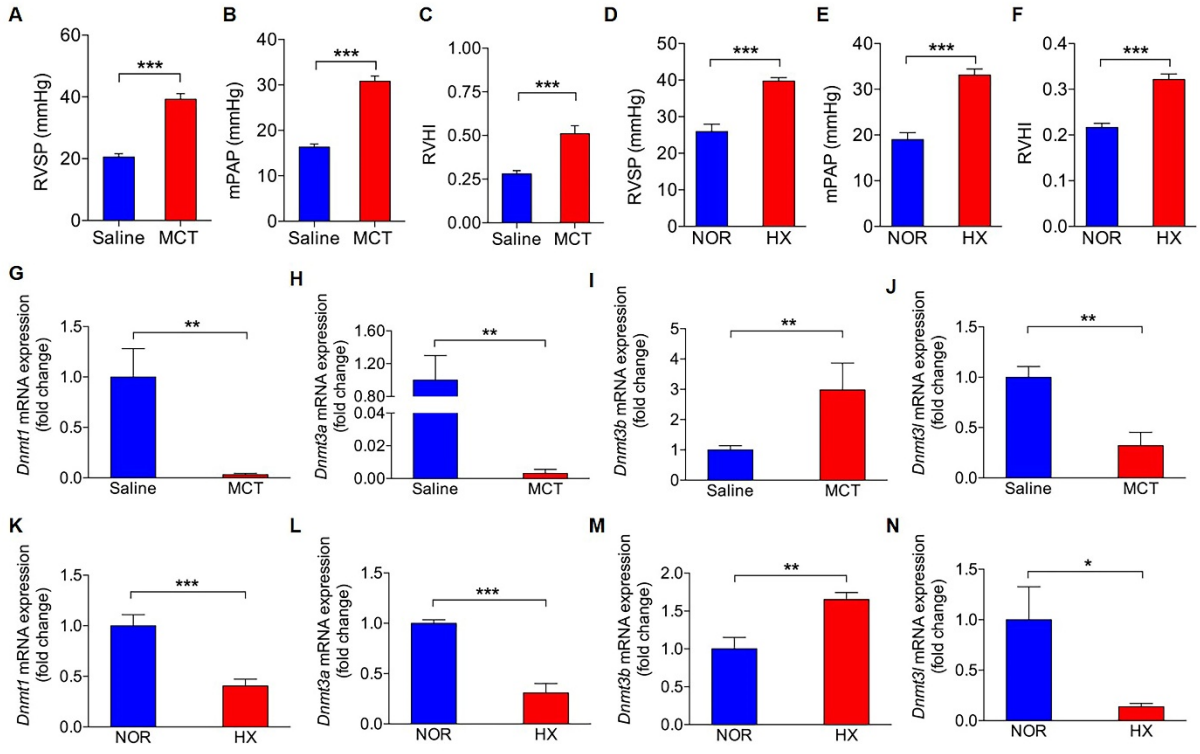

Fig. S1. DNA methyltransferases mRNA expression in lung tissues from rodent models of pulmonary hypertension.

(A-C) Sprague-Dawley rats at week 3 after MCT injection exhibited en elevation in (A) right ventricular systolic pressure (RVSP), (B) mean pulmonary arterial pressure (mPAP) and (C) right ventricular hypertrophy (RVH) assessed by the Fulton index (right ventricle / left ventricle + interventricular septum) compared to saline group (n = 7-8 per group). (D-F) Sprague-Dawley rats under hypobaric hypoxia for 3 weeks exhibited an elevation in (D) RVSP, (E) mPAP and (F) RVH assessed by the Fulton index compared to control group (n = 7-8 per group). (G-J) Sprague-Dawley rats demonstrated a reduction in (G) *Dnmt1*, (H) *Dnmt3a*, (I) *Dnmt3l* and an elevation in (J) *Dnmt3b* in lung tissues compared to saline group at mRNA level at day 21 after MCT challenge (G-J: n = 6 per group). (K-N) Sprague-Dawley rats demonstrated a reduction in (K) *Dnmt1*, (L)

Dnmt3a, (N) *Dnmt3l* and an elevation in (M) *Dnmt3b* in lung tissues compared to normobaric normoxia group at mRNA level at day 21 after exposure to hypobaric hypoxia (K-N: n = 6 per group). * $P < 0.05$, ** $P < 0.01$, *** $P < 0.001$, Student's *t*-test, mean ± SEM.

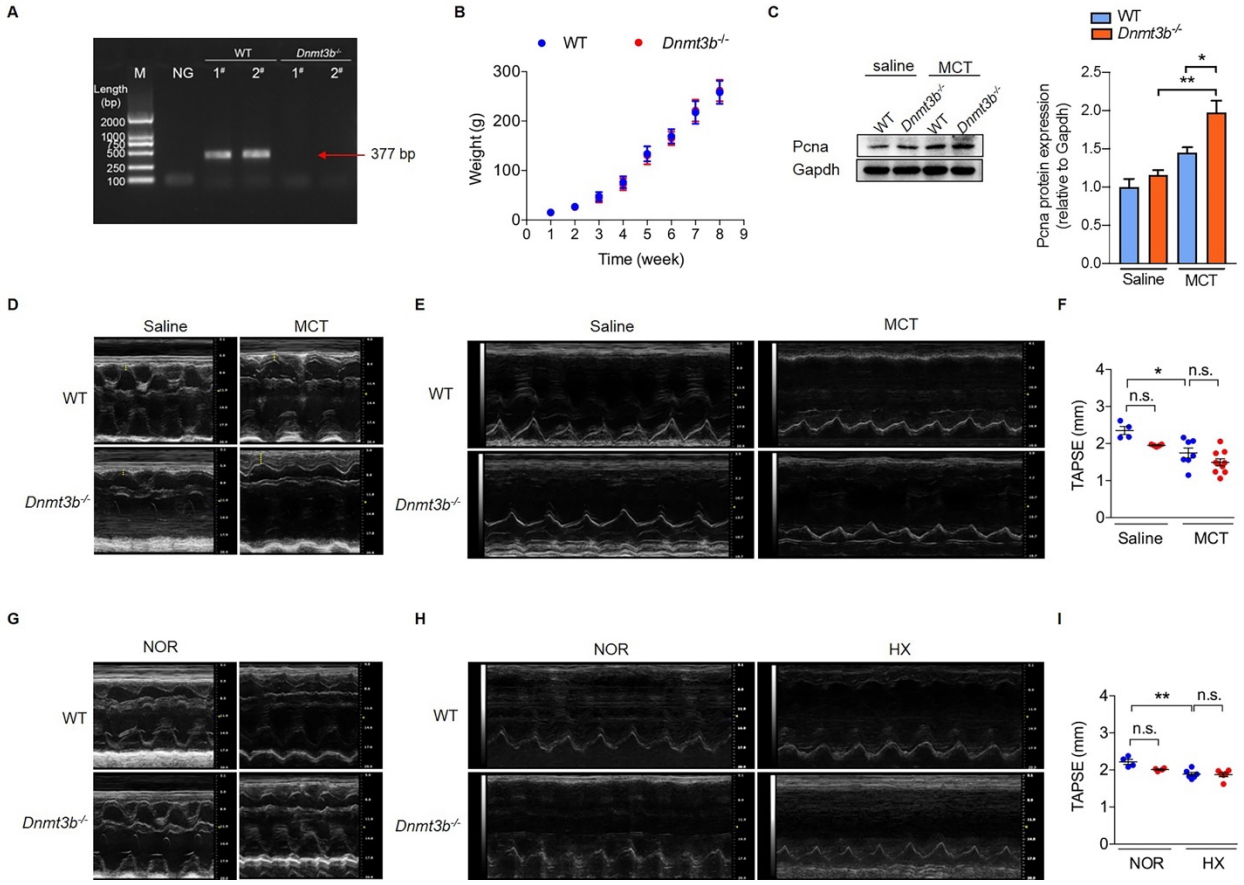

Fig. S2. Genotyping for *Dnmt3b* homozygotes and effects of Dnmt3b deficiency on proliferation, right ventricular free wall and TAPSE in rodent models of pulmonary hypertension.

(A) Representative results of a genotyping PCR using DNA from toe biopsies of homozygotes (*Dnmt3b*$^{-/-}$), and wild type rat, as well as a no template control (NG) with 1% agarose gel electrophoresis. (B) Body weights were examined between wild type and *Dnmt3b*$^{-/-}$ rats indicating that no significant difference was found between 2 groups every week after birth (n = 9 per group). (C) Pcna protein expression in lungs from MCT or saline treated *Dnmt3b*$^{-/-}$ or WT rats (n=3 per group). (D) Representative images of right ventricular free wall thickness assessed by echocardiography demonstrating that *Dnmt3b*$^{-/-}$ exhibited a thicker right ventricular free wall

compared to its littermates at day 28 after MCT challenge. (E) Representative images and (F) quantification analysis in tricuspid annular plane systolic excursion (TAPSE) assessed by echocardiography indicating that no significant difference was determined in WT and *Dnmt3b*$^{-/-}$ rats at day 28 after administration of MCT (n = 4 to 6 per group). (G) Representative images of right ventricular free wall thickness assessed by echocardiography demonstrating that *Dnmt3b*$^{-/-}$ exhibited a thicker right ventricular free wall compared to its littermates at day 21 under hypobaric hypoxic conditions. (H) Representative images and (I) quantification analysis in TAPSE assessed by echocardiography indicating that no significant difference was determined in WT and *Dnmt3b*$^{-/-}$ rats at day 21 under hypobaric hypoxic conditions (n = 4 to 6 per group). * $P < 0.05$, ** $P < 0.01$, one-way ANOVA with Bonferroni correction for multiple comparisons, mean ± SEM. n.s. indicates not significant.

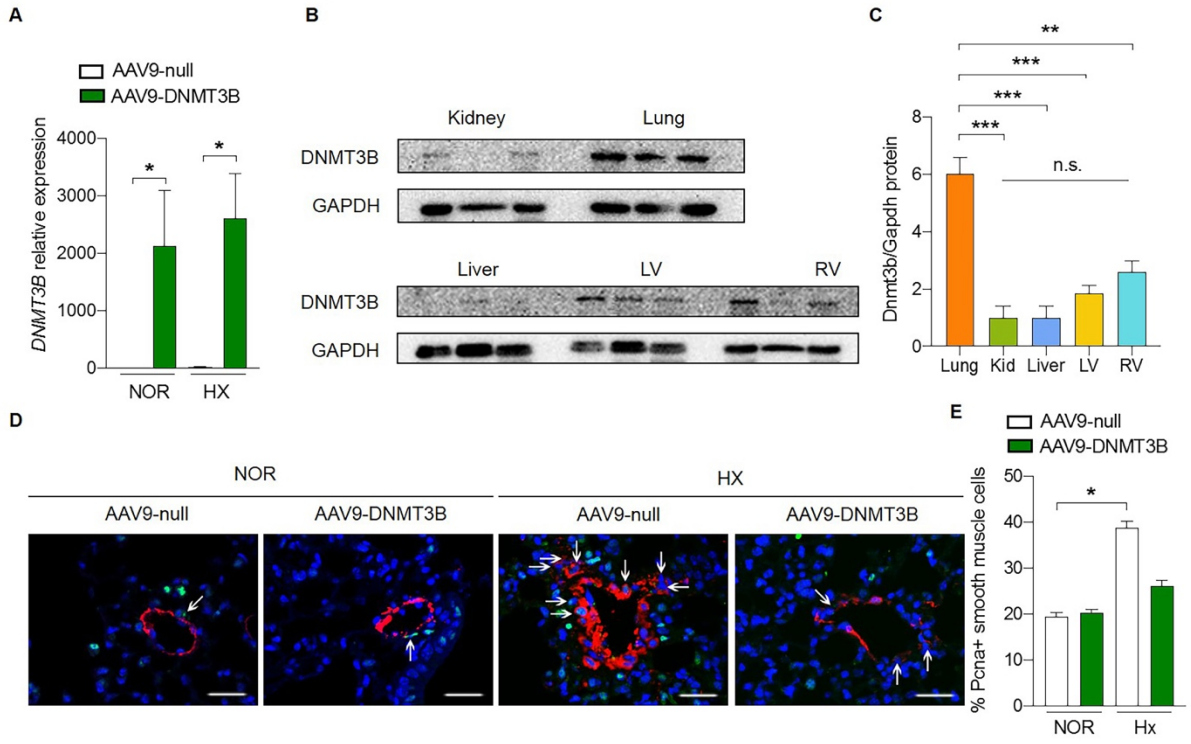

Fig. S3. DNMT3B expression and Pcna^{+} smooth muscle cells quantitative analysis in lungs of mice after intratracheal delivery of recombinant AAV9-DNMT3B.

(A) DNMT3B mRNA level in lung tissues from mice received intratracheal delivery (AAV9-DNMT3B or AAV9-null) at Day 28 under normoxia or hypoxia conditions by RT-PCR (n = 6-8 per group). (B) Representative images and (C) quantification of DNMT3B expression in different organs from AAV9-DNMT3B treated mice (n = 3). (D) Representative images and (E) quantification analysis of Pcna^{+} PASMCs in lung tissues from mice recipients (AAV9-DNMT3B or AAV9-null) at Day 28 under normoxia or hypoxia conditions by immunofluorescence co-localization (n = 3-4 per group). Scale bar: 50 μm. * $P < 0.05$, ** $P < 0.01$, *** $P < 0.001$, one-way ANOVA or Kruskal-Wallis test for multiple comparisons, mean ± SEM. n.s. indicates not significant.

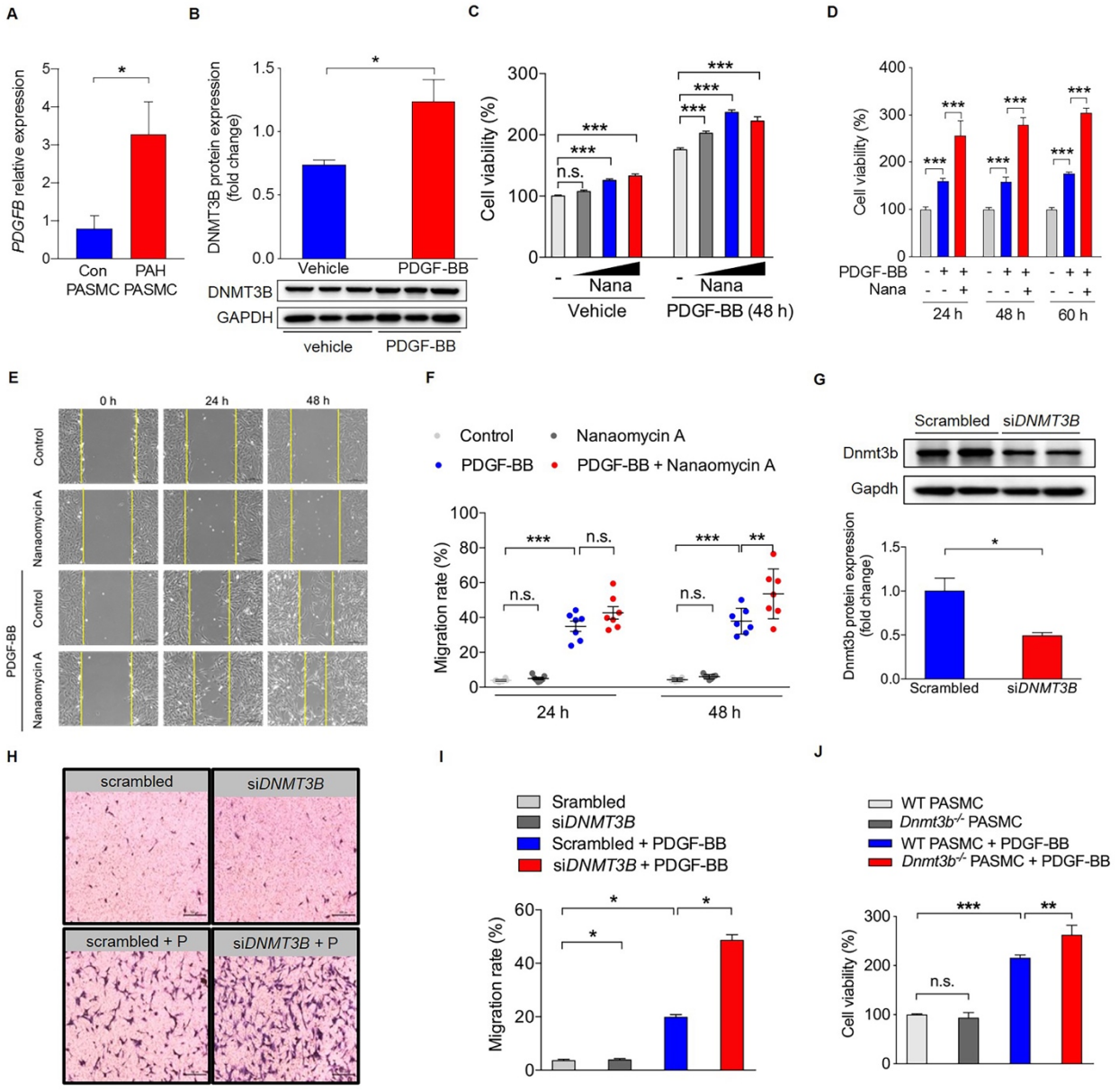

Fig. S4. PDGF-B expression and Inhibition or inactivation of Dnmt3b facilitates proliferation and migration of PASMCs respond to PDGF-BB.

(A) PDGFB mRNA expression in pulmonary arterial smooth muscle cells (PASMCs) from PAH patients (n = 5) or control subjects (n = 5). * $P < 0.05$, Student's *t*-test, mean ± SEM. (B) Immunoblotting showing increased expression of DNMT3B in human PASMCs in response to PDGF-BB for 48 h, and GAPDH was used as the loading control (lower panel). Upper panel:

Relative expression values obtained by densitometry of DNMT3B protein normalized to GAPDH. * $P < 0.05$, Student's *t*-test, mean ± SEM, $n = 3$ independent experiments. (C) Cell viability of rat PASMCs after starvation for 24 h followed by stimulation with PDGF-BB (50 ng/mL) for 48 h in the presence or absence of nanaomycin A at the indicated concentration demonstrating that nanaomycin A (0.3, 1, 3 μM) increases proliferation of PASMCs in response to PDGF-BB, and nanaomycin A (1, 3 μM) can promote rat PASMCs proliferation with no stimuli. (D) Cell viability of rat PASMCs with nanaomycin A at the concentration of 0.3 μM was higher than those without nanaomycin A treatment at 24 h, 48 h and 60 h post PDGF-BB stimulation. Values are expressed as a percentage relative to vehicle (basal medium-only) group. (E) Representative images and (F) quantification analysis of migration rate of rat PASMCs show that nanaomycin A (0.3 μM) facilitate PDGF-BB (50 ng/mL) induced rat PASMC migration by wound scratch assay. Bright-field images were obtained at ×100 magnification at 0, 24 and 48 h post-scratching. Four images of each individual scratch were taken. Scale bar: 200 μm. For statistical analysis, ** $P < 0.01$, *** $P < 0.001$ vs. vehicle or PDGF-BB treated group as indicated, one-way ANOVA with Bonferroni correction for multiple comparisons, n = 2 independent experiments. (G) Immunoblotting showing reduced expression of Dnmt3b in rat PASMCs after transfection of *Dnmt3b* siRNA for 48 h, and GAPDH was used as the loading control (upper panel). Lower panel: relative expression values obtained by densitometry of Dnmt3b protein normalized to GAPDH. * $P < 0.05$ vs. scrambled siRNA transfected rat PASMCs, Student's *t*-test, mean ± SEM, $n = 3$ independent experiments. (H) Representative images and (I) quantification analysis of migration rate of rat PASMCs show that Dnmt3b inactivation facilitate PDGF-BB (50 ng/mL)

induced rat PASMCs migration by transwell assay. Bright-field images were obtained at ×100 magnification at 18 h post-seeding in the upper chamber. Five images of each individual well were taken. Scale bar: 200 μm. For statistical analysis, * $P < 0.05$ vs. scrambled siRNA treated rat PASMCs with or without PDGF-BB stimulation as indicated, one-way ANOVA with Bonferroni correction for multiple comparisons, n = 3 independent experiments. (J) *Dnmt3b*$^{-/-}$ rat PASMCs exhibited an increased cell viability compared to wild-type (WT) PASMCs in response to PDGF-BB (50 ng/mL). Values are expressed as a percentage relative to WT control PASMCs. ** $P < 0.01$, *** $P < 0.001$ vs. WT control or WT PDGF-BB treated group as indicated, one-way ANOVA with Bonferroni correction for multiple comparisons, mean ± SEM, $n = 3$ independent experiments.

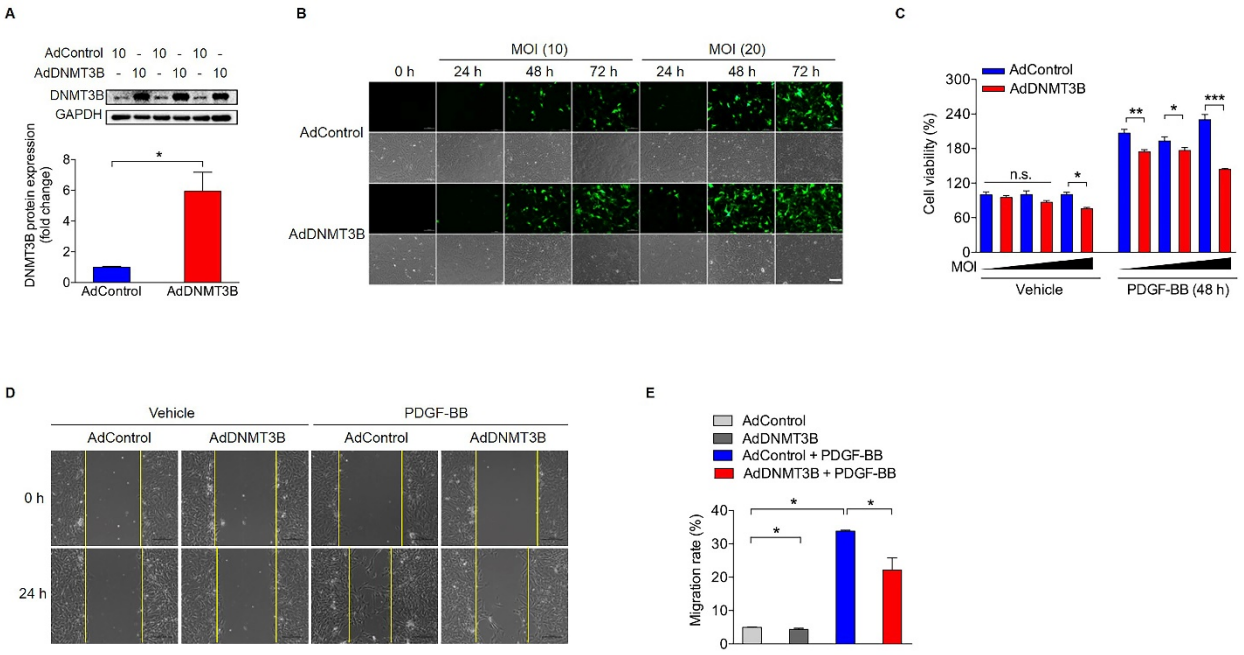

Fig. S5. DNMT3B overexpression represses proliferation and migration of rat PASMCs in response to PDGF-BB.

(A) Immunoblotting showed an elevation in DNMT3B protein level in AdDNMT3B treated human PASMCs compared to AdControl treated PASMCs at 48 h after infection (MOI=10). * $P < 0.05$ vs. AdControl treated PASMCs, Student's *t*-test, mean ± SEM, $n = 3$ independent experiments. (B) Representative images of immunofluorescence showed that DNMT3B (green, lower row) is increased in rat PASMCs after infection of Ad-DNMT3B at the indicated MOI in a time course dependent manner. Scale bar = 200 μm. (C) DNMT3B overexpression led to a reduced cell viability in rat PASMCs at the indicated MOI (10, 20, 50) at 48 h after PDGF-BB (50 ng/mL). * $P < 0.05$, ** $P < 0.01$, *** $P < 0.001$ vs. its corresponding AdControl treated without or with PDGF-BB stimuli as indicated, one-way ANOVA with Bonferroni correction for multiple comparisons, mean ± SEM, n = 3 independent experiments. (D) Representative images and (E) quantification analysis of migration rate of rat PASMCs showed that augmenting DNMT3B repressed PDGF-BB induced

rat PASMC migration by wound scratch assay. Bright-field images were obtained at × 100 magnification at 0 and 24 h post-scratching. Four images of each individual scratch were taken. Scale bar: 200 μm. For statistical analysis, * $P < 0.05$ vs. vehicle or PDGF-BB treated group as indicated, one-way ANOVA with Bonferroni correction for multiple comparisons, mean ± SEM, n = 3 independent experiments.

A

Samples	# Reads	# Retained reads	# Reads mapped to genome	Total mapping ratio (%)	# Genes
AdCon_1	24,137,141	24,103,732	21,683,847	89.96	20890
AdCon_2	24,137,454	24,098,332	21,661,962	89.89	20936
AdCon_3	24,137,103	24,062,068	21,688,565	90.14	20833
AdDNMT3B_1	24,137,021	24,102,280	21,712,656	90.09	20846
AdDNMT3B_2	24,136,951	24,072,902	21,700,483	90.14	20910
AdDNMT3B_3	24,137,095	24,096,921	21,688,362	90	20875

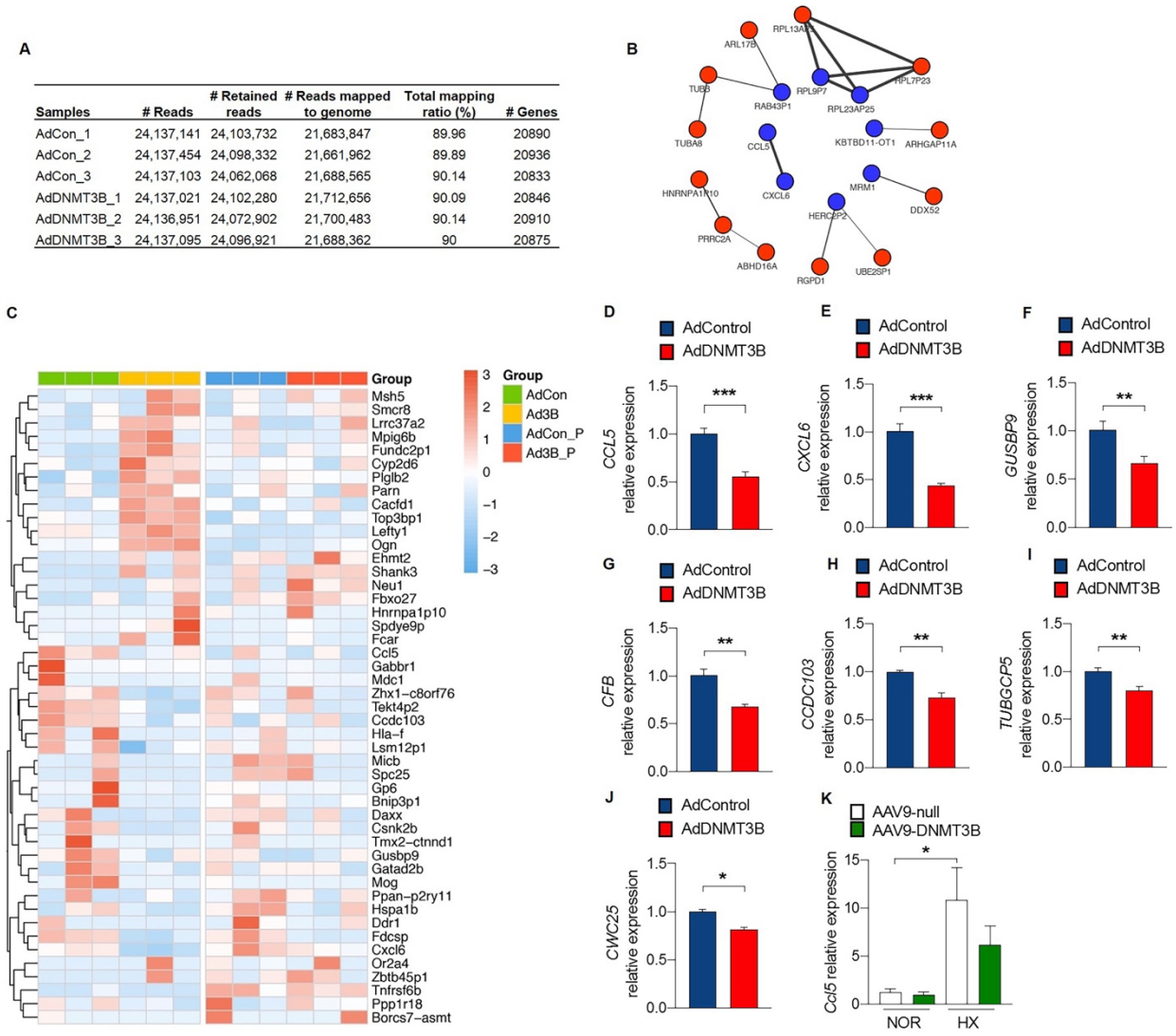

Fig. S6. RNA-seq analysis from AdDNMT3B or AdControl infected hPASMCs and verification by real time PCR in cell and animal models.

(A) Mapping statistics of AdDNMT3B vs AdControl RNA-seq data demonstrating that more than 89% of reads were mapped to the genome. (B) PPI network was construct with 20 nodes. Red nodes represent up-regulated mRNA and blue for down-regulated mRNA in AdDNMT3B infected hPASMC compared to that in AdControl group. The edge between nodes reflects interaction between genes: the wider the edge is, the stronger the interaction is. (C) Heat map illustrating

differentially expressed genes for hierarchical clustering. For AdDNMT3B infected PASMCs without (yellow bar) or with (red bar) PDGF-BB and AdControl infected PASMCs in the absence (green bar) or presence (blue bar) of PDGF-BB (n = 3 per group). (D-J) The mRNA expression of genes with asterisk in **Fig. 6d** were analyzed by RT-PCR indicating that (D) *CCL5*, (E) *CXCL6*, (F) *GUSBP9*, (G) *CFB*, (H) *CCDC103*, (I) *TUBGCP5* and (J) *CWC25* were significantly declined in human PASMCs after infection with AdDNMT3B (MOI = 20). * $P < 0.05$, ** $P < 0.01$, *** $P < 0.001$ vs. AdControl infected human PASMCs, Student's *t*-test, mean ± SEM, n = 3 independent experiments. (K) *Ccl5* mRNA expression in lungs from AAV9-DNMT3B infected mice showed a reduced trend compared to that of AAV9-null infected mice in response to hypoxia (n=6-8 per group). * $P < 0.05$ vs. AAV9-null infected mice under normoxia condition, Kruskal-Wallis test, mean ± SEM.

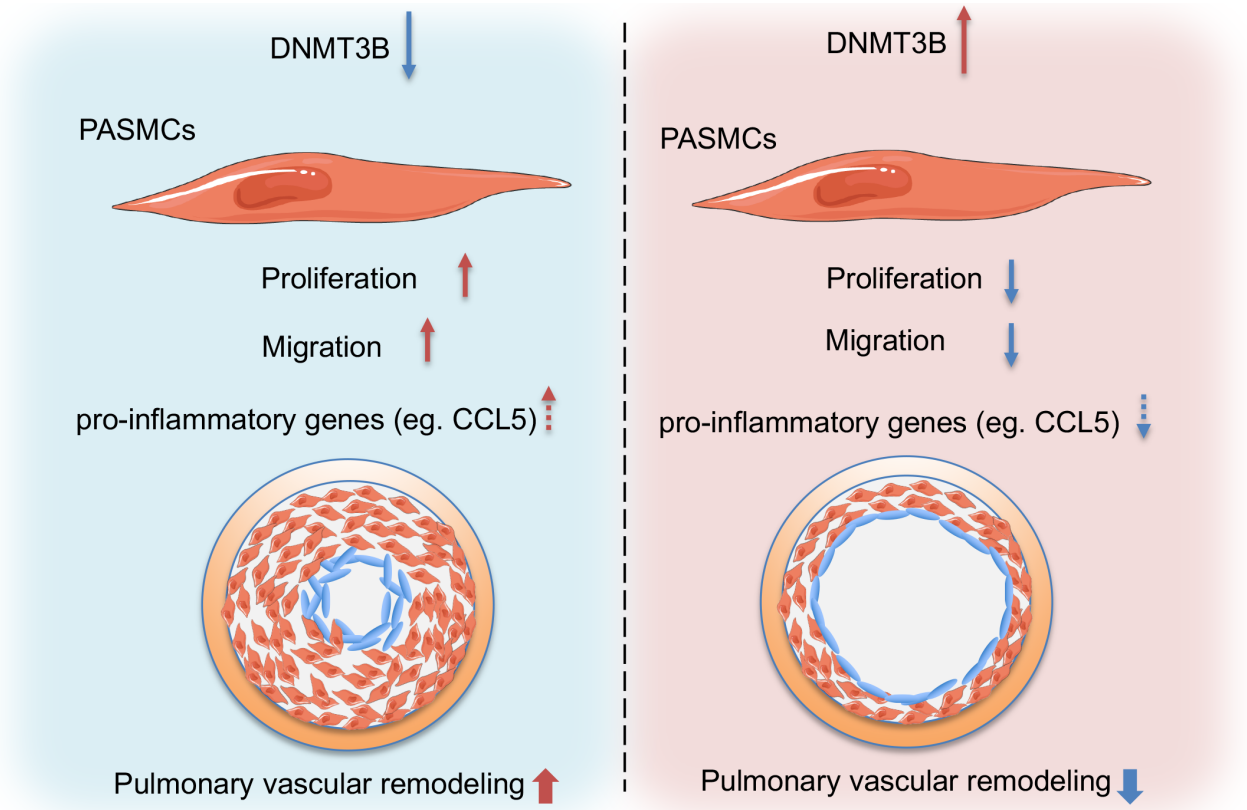

Fig. S7. Schematic of the protective role of DNMT3B in pulmonary vascular remodeling.

Pharmacological inhibition or gene-silencing of DNMT3B can promote PASMCs proliferation and migration, while excessive DNMT3B can alleviate PASMCs proliferation and migration. The process might partially link to the pro-inflammatory gene expression (eg. CCL5), which finally leads to more severe (improved) pulmonary vascular remodeling.

Table S1. Clinical data of human samples

	CHD (n=4)	CHD-PAH (n=8)	*P* value *
Age (years)	30 ± 2	26 ± 2	0.138
Gender, M/F	1/3	2/6	>0.9999
BMI (kg/m^2)	21.43 ± 2	19.47 ± 2.6	0.2828
Classification (n)			>0.9999
ASD	2	4	
VSD	2	4	
WHO FC (n)			>0.9999
I+II	3	5	
III+IV	1	3	
NT-proBNP (pg/mL)	1886 ± 763.13	2189.91 ± 1676.78	0.8485
mPAP (mm Hg)	19 ± 4	63 ± 6	0.002
PVR (Wood units)	0.76 ± 0.11	8.09 ± 0.75	<0.001
Creatinine (μmol/L)	73.87 ± 10	69.58 ± 19.93	0.3677
Bilirubin (μmol/L)	19.28 ± 4.13	20.07 ± 8.69	0.9253
Drug therapy (n)			
PDE5 inhibitors	0	3	
ERA	0	3	
CCB	0	0	
Prostanoids	0	2	

CHD: congenital heart disease; CHD-PAH: congenital heart disease associated with PAH; ASD: atrial septal defect; VSD: ventricle septal defect; WHO FC: world health organization functional

class; NT-proBNP: N-terminal pro-brain natriuretic peptide; mPAP: mean pulmonary arterial hypertension; PVR: pulmonary vascular resistance; PDE5: phosphodiesterase type 5; ERA: endothelin receptor antagonist; CCB: calcium channel blockers. Values are expressed as means and SD or frequency, as appropriate. * $P < 0.05$ vs. CHD patients.

Table S2. Differentially expressed mRNA in hPASMCs treated with AdDNMT3B for 72 h.

Gene_id	Symbol	AdCon_1	AdCon_2	AdCon_3	AdDNMT3B_1	AdDNMT3B_2	AdDNMT3B_3	Avg-AdCon	Avg-AdDNMT3B	Fold change	q-value
ENSG00000273793.3	DUSP8	19.62	23.52	2.58	0.04	0.66	0.04	15.24	0.25	0.0161854 77	2.14E-12
ENSG00000228875.8	CSNK2B	11.65	75.84	50.85	1.38	2.71	3.61	46.11	2.57	0.0556599 68	1.76E-31
ENSG00000259856.1	RAB43P1	50.06	0.04	20.15	0.04	1.88	2.62	23.42	1.51	0.0646263 35	2.54E-16
ENSG00000278670.4	GP6	1.48	1.35	29.07	0.48	1.61	0.04	10.63	0.71	0.06677116	3.61E-08
ENSG00000137403.19	HLA-F	10.91	0.31	17.67	0.89	0.74	0.78	9.63	0.80	0.0834198 68	3.86E-07

ENSG0000	MARVE									0.1337955	5.71E-1
0274671.4	LD2	24.25	50.67	31.81	12.29	1.95	0.04	35.58	4.76	59	9
ENSG0000	MBOAT									0.1459559	2.59E-3
0276935.4	7	93.8	114.42	2.46	8.24	6.88	15.63	70.23	10.25	52	4
ENSG0000	SYS1-D									0.1659440	4.18E-0
0254806.5	BNDD2	4.44	1.37	19.56	0.04	4.09	0.08	8.46	1.40	28	5
ENSG0000	HERC2P									0.1688720	2.36E-0
0280787.2	2	26.97	15.28	5.36	0.04	0.04	7.96	15.87	2.68	86	8
ENSG0000	CDH12P									0.16968421	2.57E-0
0280638.1	2	10.89	10.6	26.01	7.98	0.04	0.04	15.83	2.69	1	8
ENSG0000										0.2013685	1.18E-0
0227046.8	DAXX	12.91	25.8	2.21	1.98	3.93	2.33	13.64	2.75	24	6
ENSG0000										0.2148582	5.95E-1
0241253.8	CFB	54.16	4.27	11.43	6.66	2.22	6.13	23.29	5.00	88	0
ENSG0000	GATAD2									0.2208294	9.29E-8
0261992.2	B	0.04	414.55	285.86	59.02	95.62	0.04	233.48	51.56	67	4

ENSG0000	HIGD1A									0.2632869	4.03E-0
0227644.2	P11	15.91	12.58	8.2	0.04	8.53	1.09	12.23	3.22	99	5
ENSG0000										0.2840604	1.12E-1
0188629.11	ZNF177	52.98	36.54	40.91	2.32	26.3	8.43	43.48	12.35	16	3
ENSG0000	CCDC10									0.3360667	1.49E-0
0167131.16	3	28.11	19.8	19.16	9.94	1.39	11.21	22.36	7.51	96	6
ENSG0000	PMS2P1									0.3465467	5.52E-0
0276840.1	0	9.47	21.34	18.13	9.85	7.07	0.04	16.31	5.65	92	5
ENSG0000										0.35373711	4.40E-0
0274233.4	CCL5	42.15	20.62	30.35	3.45	10.31	19.18	31.04	10.98	3	8
ENSG0000	TUBGCP									0.3624825	3.43E-1
0276856.3	5	79.25	64.86	99.35	52.82	19.14	16.29	81.15	29.42	43	8
ENSG0000										0.3793362	1.08E-0
0215630.6	GUSBP9	13.61	31.34	21.64	10.39	0.04	14.83	22.20	8.42	37	5
ENSG0000										0.38661107	6.34E-2
0237112.8	GABBR1	266.05	39.79	39.52	47.09	39.38	47.05	115.12	44.51	3	3

ENSG0000	LSM12P									0.3961243	4.14E-1
0232024.2	1	67.95	38.11	71.46	0.04	27.25	43.03	59.17	23.44	8	2
ENSG0000	ZNF780									0.4278820	3.94E-2
0281601.2	B	35.03	215.77	261.07	155.74	20.74	42.54	170.62	73.01	79	8
ENSG0000	TEKT4P									0.4397844	2.85E-0
0188681.11	2	52.74	43.67	40.93	29.94	16.44	14.02	45.78	20.13	76	8
ENSG0000	KBTBD1									0.4449164	6.06E-1
0283239.1	1-OT1	148.37	56.2	52.04	114.09	0.04	0.04	85.54	38.06	1	4
ENSG0000										0.4451700	6.01E-0
0231179.9	MICB	38.86	19.58	15.06	4.23	8.32	20.17	24.50	10.91	68	5
ENSG0000	ZHX1-C									0.4550475	5.34E-0
0259305.6	8orf76	27.17	21.82	28.87	12.47	10.01	12.95	25.95	11.81	21	5
ENSG0000										0.4574776	3.43E-0
0215910.7	C1orf167	25.13	25.36	32.29	12.13	16.33	9.41	27.59	12.62	52	5
ENSG0000				3524.4				1922.0		0.4656256	1.24E-2
0206493.7	HLA-E	1854.11	387.5	6	1083.47	647.6	953.76	2	894.94	34	52

ENSG0000										0.4680232	1.62E-1
0124875.9	CXCL6	107	121	116	53	47	61	114.67	53.67	56	6
ENSG0000										0.4715424	3.11E-3
0283243.1	SHANK3	250	240	275	29.74	304	26.99	255.00	120.24	84	4
ENSG0000										0.4756554	9.35E-1
0181617.5	FDCSP	97	87	83	39	35	53	89.00	42.33	31	3
ENSG0000	CDC42E									0.4786629	3.03E-1
0273622.1	P5	81.31	144.89	32.27	42.53	40.6	40.59	86.16	41.24	01	2
ENSG0000										0.4901736	2.54E-2
0276761.2	CWC25	305.3	287.46	64.15	190.76	67.1	64.14	218.97	107.33	92	7
ENSG0000										2.0170627	3.44E-0
0161267.11	BDH1	12.34	21.65	15.24	57.41	26.57	15.32	16.41	33.10	67	5
ENSG0000										2.0604838	5.89E-2
0106809.10	OGN	85	76	87	160	166	185	82.67	170.33	71	2
ENSG0000	KIAA114									2.0924284	6.06E-6
0163807.5	3	394.65	329.47	12.45	545.58	773.28	222.36	245.52	513.74	18	5

ENSG0000										2.1380552	4.49E-0
0277594.2	DDX52	1.74	21.59	26.65	27.96	38.05	40.85	16.66	35.62	22	6
ENSG0000										2.2443458	2.70E-0
0215695.1	RSC1A1	30.6	13.78	0.72	45.81	14.96	40.45	15.03	33.74	98	6
ENSG0000										2.2499145	8.12E-0
0161243.8	FBXO27	2.22	2.97	53.31	2.04	24.18	105.4	19.50	43.87	3	8
ENSG0000										2.2671546	2.73E-0
0275748.4	ARL17B	23.64	0.82	19.26	19.74	37.94	41.44	14.57	33.04	2	6
ENSG0000										2.2724154	6.06E-1
0274047.4	SYNRG	190.43	571.14	218.11	1062.38	623.16	540.7	326.56	742.08	83	10
ENSG0000										2.2767686	1.56E-0
0168452.21	PPT2	19.62	16.29	26.85	32.87	99.88	10.14	20.92	47.63	42	8
ENSG0000										2.3095349	5.74E-0
0243709.1	LEFTY1	26.1	25.89	11.88	42.48	58.34	46.69	21.29	49.17	93	9
ENSG0000										2.3458953	1.03E-1
0172058.15	SERF1A	26.18	31.23	25.91	61.31	81.33	52.82	27.77	65.15	43	1

ENSG0000	FUNDC2									2.3575659	4.78E-0
0255883.1	P1	15.09	10.56	11.49	29.03	34.19	24.34	12.38	29.19	67	6
ENSG0000										2.38336611	1.08E-2
0226618.9	PRRC2A	28.32	37.42	91.89	321.95	25.53	28.21	52.54	125.23	1	1
ENSG0000	TOP3BP									2.5027995	2.46E-0
0228050.1	1	11.83	8.51	6.45	24.89	20.4	21.76	8.93	22.35	52	5
ENSG0000										2.6297715	1.04E-8
0283979.1	RFLNB	489.64	0.41	0.62	394.39	590.59	305.37	163.56	430.12	37	2
ENSG0000										2.6325190	4.72E-1
0131899.10	LLGL1	248.4	755.5	69.38	1238.85	967.14	619.44	357.76	941.81	07	79
ENSG0000										2.7925696	4.28E-0
0187994.13	RINL	21.75	3.49	3.83	40.45	34.61	6.12	9.69	27.06	59	7
ENSG0000										2.8610825	1.54E-1
0157881.13	PANK4	29.54	21.19	17.44	130.55	35.66	28.83	22.72	65.01	88	5
ENSG0000										2.8649808	8.82E-1
0176994.10	SMCR8	307.66	0.04	442.86	59.67	1107.15	983.52	250.19	716.78	14	55

ENSG0000										3.0972923	2.66E-1
0187627.15	RGPD1	8.91	20.5	14.17	51.24	57.49	26.25	14.53	44.99	36	2
ENSG0000										3.1343936	2.61E-1
0281763.2	DHX36	19.86	21.02	9.42	17.69	90.35	49.62	16.77	52.55	38	4
ENSG0000										3.20293911	3.10E-0
0183785.14	TUBA8	7.96	6.29	0.04	26	10.46	9.31	4.76	15.26	8	5
ENSG0000										3.2192050	2.45E-0
0228628.8	ATF6B	6.03	9.11	10.27	8.49	69.13	4.18	8.47	27.27	37	8
ENSG0000	GOLGA									3.3635509	8.55E-0
0278662.4	6L10	12.83	0.13	8.33	29.74	26.7	15.17	7.10	23.87	63	8
ENSG0000										3.3842923	1.16E-0
0140488.15	CELF6	0.04	9.58	14.19	28.45	24.43	27.7	7.94	26.86	14	8
ENSG0000										3.4539823	5.79E-0
0224183.1	SDHDP6	0.04	6.76	4.5	9.98	17.79	11.26	3.77	13.01	01	5
ENSG0000	LRRC37									3.6232583	5.73E-0
0274332.3	A2	4.68	0.04	13.94	25.48	26.82	15.31	6.22	22.54	07	8

ENSG0000										3.9895287	1.95E-0
0234846.7	NEU1	4.69	4.13	0.73	1.56	15.98	20.56	3.18	12.70	96	5
ENSG0000	NPHP3-									4.3297327	5.94E-3
0274810.4	ACAD11	0.04	0.04	72.13	97.02	150.66	64.97	24.07	104.22	24	7
ENSG0000										5.0351887	1.28E-1
0125551.18	PLGLB2	0.04	14.78	0.81	31.45	20.46	26.79	5.21	26.23	4	1
ENSG0000	SPDYE1									5.2719167	3.88E-0
0275976.4	1	1.76	2.76	2.21	4.4	6.79	24.29	2.24	11.83	9	6
ENSG0000	SPDYE9									5.2719167	3.88E-0
0262461.5	P	1.76	2.76	2.21	4.4	6.79	24.29	2.24	11.83	9	6
ENSG0000										5.8190045	4.83E-0
0167614.13	TTYH1	3.29	0.46	0.67	0.94	2.5	22.28	1.47	8.57	25	5
ENSG0000	ABHD16									8.7506956	2.76E-5
0204427.11	A	22.84	3.43	9.67	279.97	20.03	14.5	11.98	104.83	04	6
ENSG0000	DNMT3									9.5137931	
0088305.18	B	96	107	87	826	950	983	96.67	919.67	03	0

ENSG0000										19.573529	2.51E-1
0242852.6	ZNF709	1	0.04	1	20.01	18.92	1	0.68	13.31	41	0
ENSG0000										21.190476	1.81E-0
0172232.9	AZU1	0.04	0.04	0.97	0.95	1.73	19.57	0.35	7.42	19	6

Table S3. Primer Sequences for real time PCR

Gene symbol	Species	Forward primer	Reverse primer
GAPDH	Rattus norvegicus	CAAAGTGGACATTGTTGCCAT	AGTTGTCATATTTCTCGTGGT
DNMT1	Rattus norvegicus	GCATTACCGCAAGTATTCCG	TTGATGTCTGCCTCATTGACC
DNMT3A	Rattus norvegicus	AACTAAAACGCAGGATAGGC	TGATCAGGCTAGAGACAACCA
DNMT3B	Rattus norvegicus	CGATTCCTGGCATGTAACCC	CCCATGTTGGACACGTCT
DNMT3L	Rattus norvegicus	TCTTCCTGCTCTAAGACCCAT	TTCACGTTGACTTCGTACCTG
CCL5	Rattus norvegicus	GCTCCAACCTTGCAGTCG	TATGCCCTCCCAGGAATGAGT
CCL5	Mus musculus	TCTACACCAGCAGCAAGT	TAGGACTAGAGCAAGCAATG
GAPDH	Mus musculus	ACCTGCCAAGTATGATGAC	CTGTTGCTGTAGCCGTAT
GAPDH	Homo sapiens	TCTGACTTCAACAGCGACACC	AGCCAAATTCGTTGTCATACCAG
CCL5	Homo sapiens	ACCCGAAAGAACCGCCAA	GCCTCCCAAGCTAGGACA

CFB	Homo sapiens	TATGACGTTGCCCTGATCAAGC	GATGTAGACCTCCTTCCGAGT
CSNK2B	Homo sapiens	CAAGACGATTCGCTGATTCCC	ATTCCCACCACGATAACGACT
CXCL6	Homo sapiens	GCTGAGAGTAAACCCCAAAACGA	CCCCACACTCTTCAAAGTAGGGA
DAXX	Homo sapiens	ACGCATAGTGTCACCATCGTT	TCATGCACTGACCTTTGCCTT
DUSP8	Homo sapiens	GCAAAAGTCCTGTTCCCGTTC	CTCAGAAACCCAACGCAACAGA
GABBR1	Homo sapiens	ACTTTCTTCCGAACGCACCCAT	AGAGACGCTCCTTGTACACCT
GATAD2B	Homo sapiens	CTCCAGAAGGCATAACCC	CACGGATCATACACAAACGG
GP6	Homo sapiens	CACCACTGCACTCTAGCTC	CATTAGATGGTCAAGAAATGCCTA
HLA-E	Homo sapiens	AGCACATCTCTAGCAAATTTAGCC	CCCCACCTTTCAGTATTGCC
HLA-F	Homo sapiens	GCCCACCATCCCCATCGTG	CTGCCCCTCCTAAAGCCGAA
MARVELD2	Homo sapiens	CTAAGACCCCTTTTGTACTCG	TCACTGGTGTATTAAATAACGGAT
MBOAT7	Homo sapiens	ACTATGAGACCATCCGCAACATCG	CAGCCACCACTGCACCGTCA
MICB	Homo sapiens	CTTTCTCTTTATTCCCACGTT	TCTGTAATCCCAGCTATTCGG

SHANK3	Homo sapiens	ATCTGTGCCCTCTACAACCAG	CTGAATGGTACAACATCCGAG
C1orf167	Homo sapiens	TCCTCAGCCTTCTCCAACACA	CAAGTGCCTCCAGGATCGAA
CCDC103	Homo sapiens	GCCCCAAACCAATGAATGGAC	CCCAACCTGCACAAGAACTGA
CDC42EP5	Homo sapiens	ACACTTTAGCTCCCGGTGCAG	AGGAACGAGGTGTCCCCGAA
CWC25	Homo sapiens	TCTTGACCCGCACATTAGCTG	AAACATAATTAACCCCGGCAT
FDCSP	Homo sapiens	ATATCCATTTCGCCCACT	CCTTCTTGTTTACTTTTCGCTA
GUSBP9	Homo sapiens	CGTACCTGATGCACGAACACC	TGCCCGTAGTTGCGATACCAA
HERC2P2	Homo sapiens	ATGCCTCCTCTGTGTAGCTC	AGTCCAGAAGCCTCCATCGTT
KBTBD11-OT1	Homo sapiens	CCCATTGGCTTAAGATCCAGT	CTGTAGGCCCAATATGGTCA
SYS1-DBND2	Homo sapiens	TCCCCTAAACCATCCCGTA	AGTTTATTATTTATACCGTGCTCT
TEKT4P2	Homo sapiens	AGGAACCTCTGCACATAGCC	GACCTGCCCAGTGTCATGTCT
TUBGCP5	Homo sapiens	AGTTTCAACATCAAGTCGAGGA	ATGAGAGCCAAGTTCAACACC
ZHX1-C8orf76	Homo sapiens	GACCTGGCCTACAGACGACA	TGGACATCCCTTTTCATGGCAAA

ZNF177	Homo sapiens	TTTTCTTAACTATTTGCCCTT	ACAGGATTAGTGCAACCA
ZNF780B	Homo sapiens	CTTTCGACTTCATATGCACCT	CTCACCAGTATGAATTCGGTA
DNMT3B	Homo sapiens	CAGCCTAACACGGTGCTCA	AAACACAGAGCAGTAGCCAGT